

# Automated generation and symbolic manipulation of tensor product finite elements

Andrew T. T. McRae<sup>1,2,3,\*</sup>, Gheorghe-Teodor Bercea<sup>4</sup>,  
Lawrence Mitchell<sup>4,2</sup>, David A. Ham<sup>2,4</sup>, and Colin J. Cotter<sup>2</sup>

<sup>1</sup>*The Grantham Institute, Imperial College London, London, SW7 2AZ, UK*

<sup>2</sup>*Department of Mathematics, Imperial College London, London, SW7 2AZ, UK*

<sup>3</sup>*Department of Mathematical Sciences, University of Bath, Bath, BA2 7AY, UK*

<sup>4</sup>*Department of Computing, Imperial College London, London, SW7 2AZ, UK*

\*Correspondence to: [a.t.t.mcrae@bath.ac.uk](mailto:a.t.t.mcrae@bath.ac.uk)

We describe and implement a symbolic algebra for scalar and vector-valued finite elements, enabling the computer generation of elements with tensor product structure on quadrilateral, hexahedral and triangular prismatic cells. The algebra is implemented as an extension to the domain-specific language UFL, the Unified Form Language. This allows users to construct many finite element spaces beyond those supported by existing software packages. We have made corresponding extensions to FIAT, the FInite element Automatic Tabulator, to enable numerical tabulation of such spaces. This tabulation is consequently used during the automatic generation of low-level code that carries out local assembly operations, within the wider context of solving finite element problems posed over such function spaces. We have done this work within the code-generation pipeline of the software package Firedrake; we make use of the full Firedrake package to present numerical examples.

**Keywords:** tensor product finite element; finite element exterior calculus; automated code generation

## 1 Introduction

Many different areas of science benefit from the ability to generate approximate numerical solutions to partial differential equations. In the past decade, there has been increasing use of software packages and libraries that automate fundamental operations. The FEniCS Project (Logg et al., 2012a) is especially notable for allowing the user to express discretisations of PDEs, based on the finite element method, in UFL (Alnæs et al., 2014; Alnæs, 2012) – a concise, high-level

language embedded in Python. Corresponding efficient low-level code is automatically generated by FFC, the FEniCS Form Compiler (Kirby and Logg, 2006; Logg et al., 2012b), making use of FIAT (Kirby, 2004, 2012). These local “kernels” are executed on each cell<sup>1</sup> in the mesh, and the resulting global systems of equations can be solved using a number of third-party libraries.

There are multiple advantages to having the discretisation represented symbolically within a high-level language. The user can write down complicated expressions concisely without being encumbered by low-level implementation details. Suitable optimisations can then be applied automatically during the generation of low-level code; this would be a tedious process to replicate by hand on each new expression. Such transformations have previously been implemented in FFC (Ølgaard and Wells, 2010; Kirby and Logg, 2006). In this paper, we extend this high-level approach by introducing a user-facing symbolic representation of tensor product finite elements. Firstly, this enables the construction of a wide range of finite element spaces, particularly scalar- and vector-valued identifications of finite element differential forms. Secondly, while we have not done this at present, the symbolic representation of a tensor product finite element may be exploited to automatically generate optimal-complexity algorithms via a sum-factorisation approach.

Firedrake is an alternative software package to FEniCS which presents a similar – in many cases, identical – interface. Like FEniCS, Firedrake automatically generates low-level C kernels from high-level UFL expressions. However, the execution of these kernels over the mesh is performed in a fundamentally different way; this led to significant performance increases, relative to FEniCS 1.5, across a range of problems (Rathgeber et al., 2015). As well as the high-level representation of finite element operations embedded in Python, Firedrake and FEniCS have other attractive features. They support a wide range of arbitrary-order finite element families, which are of use to numerical analysts proposing novel discretisations of PDEs. They also make use of third-party libraries, notably PETSc (Balay et al., 2014), exposing a wide range of solvers and preconditioners for efficient solution of linear systems.

A limitation of Firedrake and FEniCS has been the lack of support for anything other than fully unstructured meshes with simplicial cells: intervals, triangles or tetrahedra. There are good reasons why a user may wish to use a mesh of non-simplicial cells. Our main motivation is geophysical simulations, which are governed by highly anisotropic equations in which gravity plays an important role. In addition, they often require high aspect-ratio domains: the vertical height of the domain may be several orders of magnitude smaller than the horizontal width. These domains admit a decomposition which has an unstructured horizontal ‘base mesh’ but with regular vertical layers – we will refer to this as an *extruded* mesh. The cells in such a mesh are not simplices but instead have a product structure. In two dimensions this leads to quadrilateral cells; in three dimensions, triangular prisms or hexahedra. From a mathematical viewpoint, the vertical alignment of cells minimises difficulties associated with the anisotropy of the governing equations. From a computational viewpoint, the vertical structure can be exploited

---

<sup>1</sup>Note on terminology: throughout this paper, we use the term ‘cell’ to denote the geometric component of the mesh; we reserve the term ‘finite element’ to denote the space of functions on a cell and supplementary information related to global continuity.

to improve performance compared to a fully unstructured mesh.

On such cells, we will focus on producing finite elements that can be expressed as (sums of) products of existing finite elements. This covers many, though not all, of the common finite element spaces on product cells. We pay special attention to element families relevant to finite element exterior calculus, a mathematical framework that leads to stable mixed finite element discretisations of partial differential equations (Arnold et al., 2006, 2010, 2014). This paper therefore describes some of the extensions to the Firedrake code-generation pipeline to enable the solution of finite element problems on cells which are products of simplices. These enable the automated generation of low-level kernels representing finite element operations on such cells. We remark that, due to our geophysical motivations, Firedrake has complete support for extruded meshes whose unstructured base mesh is built from simplices or quadrilaterals. At the time of writing, however, it does not support fully unstructured prismatic or hexahedral meshes.

Many, though not all, of the finite elements we can now construct already have implementations in other finite element libraries. `deal.II` (Bangerth et al., 2015) contains both scalar-valued tensor product finite elements and the vector-valued Raviart-Thomas and Nédélec elements of the first kind (Raviart and Thomas, 1977; Nédélec, 1980), which can be constructed using tensor products. However, `deal.II` only supports quadrilateral and hexahedral cells and has no support for simplices or triangular prisms. `DUNE PDELab` (Bastian et al., 2010) contains low-order Raviart-Thomas elements on quadrilaterals and hexahedra, but only supports scalar-valued elements on triangular prisms. `Nektar++` (Cantwell et al., 2015) uses tensor-product elements extensively and supports a wide range of geometric cells, but is restricted to scalar-valued finite elements. `MFEM` (mfe) supports Raviart-Thomas and Nédélec elements of the first kind, though it has no support for triangular prisms. `NGSolve` (Schöberl, 2014; Schöberl and Zaglmayr, 2005) contains many, possibly all, of the exterior-calculus-inspired tensor-product elements that we can create on triangular prisms and hexahedra. However, it does not support elements such as the Nédélec element of the second kind (Nédélec, 1986) on these cells, which do not fit into the exterior calculus framework.

This paper is structured as follows: in section 2, we provide the mathematical details of product finite elements. In section 3, we describe the software extensions that allow such elements to be represented and numerically tabulated. In section 4, we present numerical experiments that make use of these elements, within Firedrake. Finally, in section 5 and section 6, we give some limitations of our implementation and other closing remarks.

## 1.1 Summary of contributions

- The description and implementation of a symbolic algebra on existing scalar- and vector-valued finite elements. This allows for the creation of scalar-valued continuous and discontinuous tensor product elements, and vector-valued curl- and div-conforming tensor product elements in two and three dimensions.
- Certain vector-valued finite elements on quadrilaterals, triangular prisms and hexahedra are completely unavailable in other major packages, and some elements we create have

no previously published implementation.

- The tensor product element structure is captured symbolically at runtime. Although we do not take advantage of this at present, this could later be exploited to automate the generation of low-complexity algorithms through sum-factorisation and similar techniques.

## 2 Mathematical preliminaries

This section is structured as follows: in subsection 2.1, we give the definition of a finite element that we work with. In subsection 2.2, we briefly define the sum of finite elements. In subsection 2.3, we discuss finite element spaces in terms of their inter-cell continuity. In subsection 2.4 and subsection 2.5, which form the main part of this section, we define the product of finite elements and state how these products can be manipulated and combined to produce elements compatible with finite element exterior calculus. Up to this point, our exposition uses the language of scalar and vector fields as our existing software infrastructure uses scalars and vectors and we believe this makes the paper accessible to a wider audience. However, we end this section with subsection 2.6, which briefly re-states subsection 2.4 and subsection 2.5 in terms of differential forms. These provide a far more natural setting for the underlying operations.

### 2.1 Definition of a finite element

We will follow Ciarlet (1978) in defining a *finite element* to be a triple  $(K, P, N)$  where

- $K$  is a bounded domain in  $\mathbb{R}^n$ , to be interpreted as a generic *reference cell* on which all calculations are performed,
- $P$  is a finite-dimensional space of continuous functions on  $K$ , typically some subspace of polynomials,
- $N = \{n_1, \dots, n_{\dim P}\}$  is a basis for the dual space  $P'$  – the space of linear functionals on  $P$  – where the elements of the set  $N$  are called *nodes*.

Let  $\Omega$  be a compact domain which is decomposed into a finite number of non-overlapping cells. Assume that we wish to find an approximate solution to some partial differential equation, posed in  $\Omega$ , using the finite element method. A *finite element* together with a given decomposition of  $\Omega$  produce a *finite element space*.

A finite element space is a finite-dimensional function space on  $\Omega$ . There are essentially two things that need to be specified to characterise a finite element space: the manner in which a function may vary within a single cell, and the amount of continuity a function must have between neighbouring cells.

The former is related to  $P$ ; more details are given in subsection 2.3.2. A basis for  $P$  is therefore very useful in implementations of the finite element method. Often, this is a *nodal basis* in which each of the basis functions  $\Phi_1, \dots, \Phi_{\dim P}$  vanish when acted on by all but one

node:

$$n_i(\Phi_j) = \delta_{ij}. \quad (2.1)$$

Basis functions from different cells can be combined into basis functions for the finite element space on  $\Omega$ . The inter-cell continuity of these basis functions is related to the choice of nodes,  $N$ . This is the core topic of subsection 2.3.

## 2.2 Sum of finite elements

Suppose we have finite elements  $U = (K, P_A, N_A)$  and  $V = (K, P_B, N_B)$ , which are defined over the same reference cell  $K$ . If the intersection of  $P_A$  and  $P_B$  is trivial, we can define the *direct sum*  $U \oplus V$  to be the finite element  $(K, P, N)$ , where

$$P := P_A \oplus P_B \equiv \{f_A + f_B \mid f_A \in P_A, f_B \in P_B\} \quad (2.2)$$

$$N := N_A \cup N_B. \quad (2.3)$$

## 2.3 Sobolev spaces, inter-cell continuity, and Piola transforms

Finite element spaces are a finite-dimensional subspace of some larger Sobolev space, depending on the degree of continuity of functions between neighbouring cells. We will consider finite element spaces in  $H^1$ ,  $H(\text{curl})$ ,  $H(\text{div})$  and  $L^2$ .

A brief remark: it is clear that these Sobolev spaces have some trivial inclusion relations –  $H^1$  is a subspace of  $L^2$ ,  $H(\text{div})$  and  $H(\text{curl})$  are both subspaces of  $[L^2]^d$ , where  $d$  is the spatial dimension, and  $[H^1]^d$  is a subspace of both  $H(\text{div})$  and  $H(\text{curl})$ . However, in what follows, when we make casual statements such as  $V \subset H(\text{div})$ , it is *implied* that  $V \not\subset [H^1]^d$ , i.e., we have made the strongest statement possible. In particular, we will use  $L^2$  to denote a total absence of continuity between cells.

### 2.3.1 Geometric decomposition of nodes

The set of nodes  $N$ , from the definition in subsection 2.1, are used to enforce the continuity requirements on the ‘global’ finite element space. This is done by associating nodes with *topological* entities of  $K$  – vertices, facets, and so on. When multiple cells in  $\Omega$  share a topological entity, the cells must agree on the value of any degree of freedom associated with that entity. This leads to coupling between any cells that share the entity. The association of nodes with topological entities is crucial in determining the continuity of finite element spaces – this is sometimes called the *geometric decomposition* of nodes.

For  $H^1$  elements, functions are fully continuous between cells, and must therefore be single-valued on vertices, edges and facets. Nodes are firstly associated with *vertices*. If necessary, additional nodes are associated with *edges*, then with *facets*, then with the *interior* of the reference cell.

For  $H(\text{curl})$  elements, which are intrinsically vector-valued, functions must have continuous tangential component between cells. The component(s) of the function tangential to edges and facets must therefore be single-valued. Nodes are firstly associated with *edges* until the tangential component is specified uniquely. If necessary, additional nodes are associated with *facets*, then with the *interior* of the reference cell.

For  $H(\text{div})$  elements, which are also intrinsically vector-valued, functions must have continuous normal component between cells. The component of the function normal to facets must therefore be single-valued. Nodes are firstly associated with *facets*. If necessary, additional nodes are associated with the *interior* of the cell.

$L^2$  elements have no continuity requirements. Typically, all nodes are associated with the *interior* of the cell; this does not lead to any continuity constraints.

### 2.3.2 Piola transforms

For functions to have the desired continuity on the global mesh, they may need to undergo an appropriate *mapping* from reference to physical space. Let  $\vec{X}$  represent coordinates on the reference cell, and  $\vec{x}$  represent coordinates on the physical cell; for each physical cell there is some map  $\vec{x} = g(\vec{X})$ .

For  $H^1$  or  $L^2$  functions, no explicit mapping is needed. Let  $\hat{f}(\vec{X})$  be a function defined over the reference cell. The corresponding function  $f(\vec{x})$  defined over the physical cell is then

$$f(\vec{x}) = \hat{f} \circ g^{-1}(\vec{x}). \quad (2.4)$$

We will refer to this as the *identity* mapping.

However, if we wish to have continuity of the normal or tangential component of the vector field in physical space; Eq. (2.4) does not suffice.  $H(\text{div})$  and  $H(\text{curl})$  elements therefore use *Piola transforms* to map functions from reference space to physical space. We will use  $J$  to denote  $Dg(\vec{X})$ , the Jacobian of the coordinate transformation.  $H(\text{div})$  functions are mapped using the contravariant Piola transform, which preserves normal components:

$$\vec{f}(\vec{x}) = \frac{1}{\det J} J \hat{f} \circ g^{-1}(\vec{x}), \quad (2.5)$$

while  $H(\text{curl})$  functions are mapped using the covariant Piola transform, which preserves tangential components:

$$\vec{f}(\vec{x}) = J^{-T} \hat{f} \circ g^{-1}(\vec{x}). \quad (2.6)$$

## 2.4 Product finite elements

In this section, we discuss how to take the product of a pair of finite elements and how this product element may be manipulated to give different types of inter-cell continuity. We will label our constituent elements  $U$  and  $V$ , where  $U := (K_A, P_A, N_A)$  and  $V := (K_B, P_B, N_B)$  following the

notation of subsection 2.1. We begin with the definition of the product reference cell, which is straightforward. However, the spaces of functions and the associated nodes are intimately related, hence the discussion of these is interleaved.

### 2.4.1 Product cells

Given reference cells  $K_A \subset \mathbb{R}^n$  and  $K_B \subset \mathbb{R}^m$ , the reference product cell  $K_A \times K_B$  can be defined straightforwardly as follows:

$$K_A \times K_B := \{(x_1, \dots, x_{n+m}) \in \mathbb{R}^{n+m} \mid (x_1, \dots, x_n) \in K_A, (x_{n+1}, \dots, x_{n+m}) \in K_B\}. \quad (2.7)$$

The topological entities of  $K_A \times K_B$  correspond to products of topological entities of  $K_A$  and  $K_B$ . If we label the entities of a reference cell (in  $\mathbb{R}^n$ , say) by their dimension, so that 0 corresponds to vertices, 1 to edges,  $\dots$ ,  $n-1$  to facets and  $n$  to the cell, the entities of  $K_A \times K_B$  can be labelled as follows:

**(0, 0):** vertices of  $K_A \times K_B$  – the product of a vertex of  $K_A$  with a vertex of  $K_B$

**(1, 0):** edges of  $K_A \times K_B$  – the product of an edge of  $K_A$  with a vertex of  $K_B$

**(0, 1):** edges of  $K_A \times K_B$  – the product of a vertex of  $K_A$  with an edge of  $K_B$

$\vdots$

**(n-1, m):** facets of  $K_A \times K_B$  – the product of a facet of  $K_A$  with the cell of  $K_B$

**(n, m-1):** facets of  $K_A \times K_B$  – the product of the cell of  $K_A$  with a facet of  $K_B$

**(n, m):** cell of  $K_A \times K_B$  – the product of the cell of  $K_A$  with the cell of  $K_B$

It is important to distinguish between different types of entities, even those with the same dimension. For example, if  $K_A$  is a triangle and  $K_B$  an interval, the  $(2, 0)$  facets of the prism  $K_A \times K_B$  are triangles while the  $(1, 1)$  facets are quadrilaterals.

### 2.4.2 Product spaces of functions – simple elements

Given spaces of functions  $P_A$  and  $P_B$ , the product space  $P_A \otimes P_B$  can be defined as the span of products of functions in  $P_A$  and  $P_B$ :

$$P_A \otimes P_B := \text{span}\{f \cdot g \mid f \in P_A, g \in P_B\}, \quad (2.8)$$

where the product function  $f \cdot g$  is defined so that

$$(f \cdot g)(x_1, \dots, x_{n+m}) = f(x_1, \dots, x_n) \cdot g(x_{n+1}, \dots, x_{n+m}). \quad (2.9)$$

In the cases we consider explicitly, at least one of  $f$  or  $g$  will be scalar-valued, so the product on the right-hand side of Eq. (2.9) is unambiguous. A basis for  $P_A \otimes P_B$  can be constructed from bases for  $P_A$  and  $P_B$ . If  $P_A$  and  $P_B$  have nodal bases

$$\{\Phi_1^{(A)}, \Phi_2^{(A)}, \dots, \Phi_N^{(A)}\}, \{\Phi_1^{(B)}, \Phi_2^{(B)}, \dots, \Phi_M^{(B)}\} \quad (2.10)$$

respectively, a nodal basis for  $P_A \otimes P_B$  is given by

$$\{\Phi_{i,j}, \quad i = 1, \dots, N, j = 1, \dots, M\}, \quad (2.11)$$

where

$$\Phi_{i,j} := \Phi_i^{(A)} \cdot \Phi_j^{(B)}, \quad i = 1, \dots, N, j = 1, \dots, M; \quad (2.12)$$

the right-hand side uses the same product as Eq. (2.9).

While this already gives plenty of flexibility, there are cases in which a different, more natural, space can be built by further manipulation of  $P_A \otimes P_B$ . We will return to this after a brief description of product nodes.

### 2.4.3 Product nodes – geometric decomposition

Recall that the nodes are a basis for the dual space  $(P_A \otimes P_B)'$ , and that the inter-cell continuity of the finite element space is related to the association of nodes with topological entities of the reference cell.

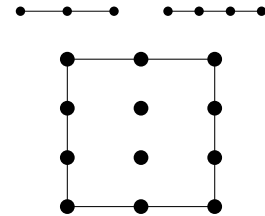
Assuming that we know bases for  $P'_A$  and  $P'_B$ , there is a natural basis for  $(P_A \otimes P_B)'$  which is essentially an outer (tensor) product of the bases for  $P'_A$  and  $P'_B$ . Let  $n_{i,j}$  denote a “product” of  $n_i^{(A)}$ , the  $i$ 'th node in  $N_A$ , with  $n_j^{(B)}$ , the  $j$ 'th node in  $N_B$  – typically the evaluation of some component of the function. If  $n_i^{(A)}$  is associated with an entity of  $K_A$  of dimension  $p$  and  $n_j^{(B)}$  is associated with an entity of  $K_B$  of dimension  $q$  then  $n_{i,j}$  is associated with an entity of  $K_A \times K_B$  with label  $(p, q)$ .

This geometric decomposition of nodes in the product element is used to motivate further manipulation of  $P_A \otimes P_B$  to produce a more natural space of functions, particularly in the case of vector-valued elements.

### 2.4.4 Product spaces of functions – scalar- and vector-valued elements in 2D and 3D

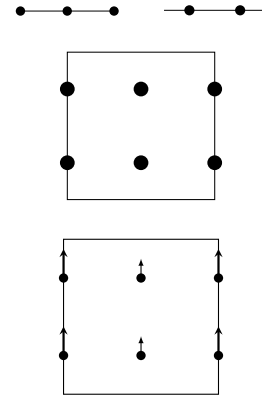
In two dimensions, we take the reference cells  $K_A$  and  $K_B$  to be intervals, so the product cell  $K_A \times K_B$  is two-dimensional. Finite elements on intervals are scalar-valued and are either in  $H^1$  or  $L^2$ . We will consider the creation of two-dimensional elements in  $H^1$ ,  $H(\text{curl})$ ,  $H(\text{div})$  and  $L^2$ . A summary of the following is given in Table 1.

$H^1$ : The element must have nodes associated with vertices of the reference product cell. The vertices of the reference product cell are formed by taking the product of vertices on the intervals. The constituent elements must therefore have nodes associated with vertices, so must both be in  $H^1$ .



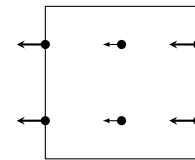


$H(\text{curl})$ : The element must have nodes associated with edges of the reference product cell. The edges of the reference product cell are formed by taking the product of an interval's vertex with an interval's interior. One of the constituent elements must therefore have nodes associated with vertices, while the other must only have nodes associated with the interior. Taking the product of an  $H^1$  element with an  $L^2$  element gives a scalar-valued element with nodes on the  $(0, 1)$  facets, for example.



To create an  $H(\text{curl})$  element, we now multiply this scalar-valued element by the vector  $(0, 1)$  to create a vector-valued finite element (if we had taken the product of an  $L^2$  element with an  $H^1$  element, we would multiply by  $(1, 0)$ ). This gives an element whose tangential component is continuous across *all* edges (trivially so on two of the edges). In addition, we must use an appropriate Piola transform when mapping from reference space into physical space.

$H(\text{div})$ : We create a scalar-valued element in the same way as in the  $H(\text{curl})$  case, but multiplied by the 'other' basis vector (for  $H^1 \times L^2$ , we choose  $(-1, 0)$  – the minus sign is useful for orientation consistency in unstructured quadrilateral meshes; for  $L^2 \times H^1$ ,  $(0, 1)$ ). This gives an element whose normal component is continuous across *all* edges, and again, we must use an appropriate Piola transform when mapping from reference space into physical space.



Note that the scalar-valued product elements we produce above are perfectly legitimate finite elements, and it is not compulsory to form vector-valued elements from them. Indeed, we use such a scalar-valued element for the example in subsection 4.2. However, the vector-valued elements are generally more useful and fit naturally within Finite Element Exterior Calculus, as we will see in subsection 2.5.

$L^2$ : The element must only have nodes associated with interior of the reference product cell. The constituent elements must therefore only have nodes associated with their interiors, so must both be in  $L^2$ .

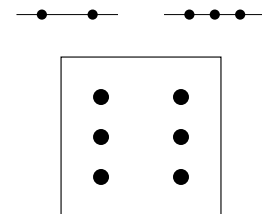


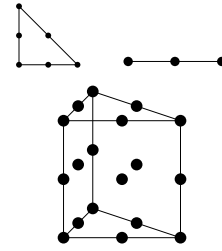
Table 1: Summary of 2D product elements

Product (1D $\times$ 1D)	Components	Modifier	Result	Mapping
$H^1 \times H^1$	$f \times g$	(none)	$fg$	identity
$H^1 \times L^2$	$f \times g$	(none)	$fg$	identity
$H^1 \times L^2$	$f \times g$	$H(\text{curl})$	$(0, fg)$	covariant Piola
$H^1 \times L^2$	$f \times g$	$H(\text{div})$	$(-fg, 0)$	contravariant Piola
$L^2 \times H^1$	$f \times g$	(none)	$fg$	identity
$L^2 \times H^1$	$f \times g$	$H(\text{curl})$	$(fg, 0)$	covariant Piola
$L^2 \times H^1$	$f \times g$	$H(\text{div})$	$(0, fg)$	contravariant Piola
$L^2 \times L^2$	$f \times g$	(none)	$fg$	identity

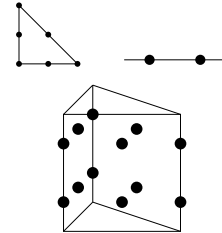
In three dimensions, we take  $K_A \subset \mathbb{R}^2$  and  $K_B$  to be an interval, so the product cell  $K_A \times K_B$  is three-dimensional. Finite elements on a 2D reference cell may be in  $H^1$ ,  $H(\text{curl})$ ,  $H(\text{div})$  or  $L^2$ . Elements on a 1D reference cell may be in  $H^1$  or  $L^2$ . We will consider the creation of three-dimensional elements in  $H^1$ ,  $H(\text{curl})$ ,  $H(\text{div})$  and  $L^2$ . A summary of the following is given in Table 2.

*Note: In the following pictures, we have taken the two-dimensional cell to be a triangle. However, the discussion is equally valid for quadrilaterals.*

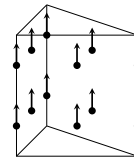
$H^1$ : As in the two-dimensional case, this is formed by taking the product of two  $H^1$  elements.



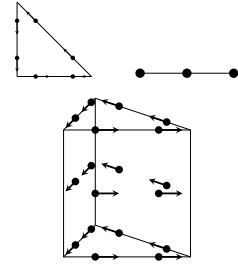
$H(\text{curl})$ : The element must again have nodes associated with edges of the reference product cell. There are two distinct ways of forming such an element, and in both cases a suitable Piola transform must be used to map functions from reference to physical space.



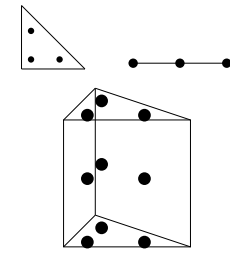
Taking the product of an  $H^1$  two-dimensional element with an  $L^2$  one-dimensional element produces a scalar-valued element with nodes on  $(0, 1)$  edges. If we multiply this by the vector  $(0, 0, 1)$ , this results in an element whose tangential component is continuous on all edges and faces.



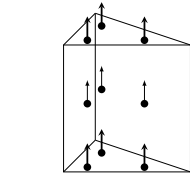
Alternatively, one may take the product of an  $H(\text{div})$  or  $H(\text{curl})$  two-dimensional element with an  $H^1$  one-dimensional element. This produces a vector-valued element with nodes on  $(1,0)$  edges. The product naturally takes values in  $\mathbb{R}^2$ , since the two-dimensional element is vector-valued and the one-dimensional element is scalar-valued. However, an  $H(\text{curl})$  element in three dimensions must take values in  $\mathbb{R}^3$ . If the two-dimensional element is in  $H(\text{curl})$ , it is enough to interpret the product as the first two components of a three-dimensional vector. If the two-dimensional element is in  $H(\text{div})$ , the two-dimensional product must be *rotated* by 90 degrees before being transformed into a three-dimensional vector.



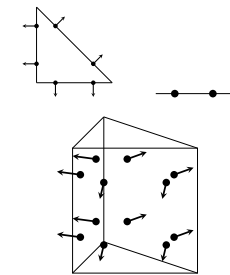
$H(\text{div})$ : The element must have nodes associated with facets of the reference product cell. As with  $H(\text{curl})$ , there are two distinct ways of forming such an element, and suitable Piola transforms must again be used.



Taking the product of an  $L^2$  two-dimensional element with an  $H^1$  one-dimensional element gives a scalar-valued element with nodes on  $(2,0)$  facets. Multiplying this by  $(0,0,1)$  produces an element whose normal component is continuous across all facets.



Taking the product of an  $H(\text{div})$  or  $H(\text{curl})$  two-dimensional element with an  $L^2$  one-dimensional element gives a vector-valued element with nodes on  $(1,1)$  facets. Again, the product naturally takes values in  $\mathbb{R}^2$ . If the two-dimensional element is in  $H(\text{div})$ , it is enough to interpret the product as the first two components of a three-dimensional vector-valued element whose third component vanishes. If the two-dimensional element is in  $H(\text{curl})$ , the product must be rotated by 90 degrees before transforming.



$L^2$ : As in the 2D case, both constituent elements must be in  $L^2$ .

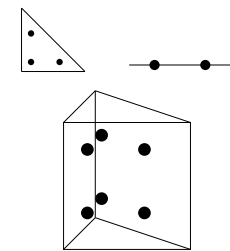


Table 2: Summary of 3D product elements

Product (2D $\times$ 1D)	Components	Modifier	Result	Mapping
$H^1 \times H^1$	$f \times g$	(none)	$fg$	identity
$H^1 \times L^2$	$f \times g$	(none)	$fg$	identity
$H^1 \times L^2$	$f \times g$	$H(\text{curl})$	$(0, 0, fg)$	covariant Piola
$H(\text{curl}) \times H^1$	$(f_x, f_y) \times g$	(none)	$(f_x g, f_y g)^\dagger$	*
$H(\text{curl}) \times H^1$	$(f_x, f_y) \times g$	$H(\text{curl})$	$(f_x g, f_y g, 0)$	covariant Piola
$H(\text{div}) \times H^1$	$(f_x, f_y) \times g$	(none)	$(f_x g, f_y g)^\dagger$	*
$H(\text{div}) \times H^1$	$(f_x, f_y) \times g$	$H(\text{curl})$	$(-f_y g, f_x g, 0)$	covariant Piola
$H(\text{curl}) \times L^2$	$(f_x, f_y) \times g$	(none)	$(f_x g, f_y g)^\dagger$	*
$H(\text{curl}) \times L^2$	$(f_x, f_y) \times g$	$H(\text{div})$	$(f_y g, -f_x g, 0)$	contravariant Piola
$H(\text{div}) \times L^2$	$(f_x, f_y) \times g$	(none)	$(f_x g, f_y g)^\dagger$	*
$H(\text{div}) \times L^2$	$(f_x, f_y) \times g$	$H(\text{div})$	$(f_x g, f_y g, 0)$	contravariant Piola
$L^2 \times H^1$	$f \times g$	(none)	$fg$	identity
$L^2 \times H^1$	$f \times g$	$H(\text{div})$	$(0, 0, fg)$	contravariant Piola
$L^2 \times L^2$	$f \times g$	(none)	$fg$	identity

The elements marked with  $^\dagger$  are of little practical use; they are 2-vector valued but are defined over three-dimensional domains. No mapping has been given for these elements; the Piola transformations from a 3D cell require all three components to be defined.

#### 2.4.5 Consequences for implementation

The previous subsections motivate the implementation of several mathematical operations on finite elements. We will need an operator that takes the product of two existing elements; we call this `TensorProductElement`. This will generate a new element whose reference cell is the product of the reference cells of the constituent elements, as described in subsection 2.4.1. It will also construct the product space of functions  $P_A \otimes P_B$ , as described in subsection 2.4.2, but with no extra manipulation (e.g. expanding into a vector-valued space). The basis for  $P_A \otimes P_B$  is as defined in Eqs. (2.11) and (2.12). The nodes are topologically associated with topological entities of the reference cell as described in subsection 2.4.3.

To construct the more complicated vector-valued finite elements, we introduce additional operators `HCurl` and `HDiv` which form a vector-valued  $H(\text{curl})$  or  $H(\text{div})$  element from an existing `TensorProductElement`. This will modify the product space as described in subsection 2.4.4 by manipulating the existing product into a vector of the correct dimension (after rotation, if applicable), and setting an appropriate Piola transform. We will also need an operator that creates the sum of finite elements; this already exists in UFL under the name `EnrichedElement`, and is represented by `+`.

### 2.5 Product finite elements within finite element exterior calculus

The work of Arnold et al. (2006, 2010) on finite element exterior calculus provides principles for obtaining stable mixed finite element discretisations on a domain consisting of simplicial cells: intervals, triangles, tetrahedra, and higher-dimensional analogues. In full generality, this involves de Rham complexes of polynomial-valued finite element differential forms linked by

the exterior derivative operator. In 1, 2 and 3 dimensions, differential forms can be naturally identified with scalar and vector fields, while the exterior derivative can be interpreted as a standard differential operator such as grad, curl, or div. The vector-valued element spaces only have partial continuity between cells: they are in  $H(\text{curl})$  or  $H(\text{div})$ , which have been discussed already. The element spaces themselves were, however, already well-known in the existing finite element literature for their use in solving mixed formulations of the Poisson equation and problems of a similar nature.

Arnold et al. (2014) generalises finite element exterior calculus to cells which can be expressed as geometric products of simplices. It also describes a specific complex of finite element spaces on hexahedra (and, implicitly, quadrilaterals). When these differential forms are identified with scalar- and vector-valued functions, they correspond to the scalar-valued  $Q_r$  and its discontinuous counterpart  $DQ_r$ , and various well-known vector-valued spaces as introduced in Brezzi et al. (1985), Nédélec (1980) and Nédélec (1986). Within finite element exterior calculus, there are element spaces which cannot be expressed as a tensor product of spaces on simplices – see, for example, Arnold and Awanou (2014) – but we are not considering such spaces in this paper.

Finite element exterior calculus makes use of de Rham complexes of finite element spaces. In one dimension, the complex takes the form

$$U_0 \xrightarrow{\frac{d}{dx}} U_1, \quad (2.13)$$

where  $U_0 \subset H^1$  and  $U_1 \subset L^2$ . In two dimensions, there are two types of complex, arising due to two possible identifications of differential 1-forms with vector fields:

$$U_0 \xrightarrow{\nabla^\perp} U_1 \xrightarrow{\nabla \cdot} U_2, \quad (2.14)$$

where  $U_0 \subset H^1$ ,  $U_1 \subset H(\text{div})$ , and  $U_2 \subset L^2$ , and

$$U_0 \xrightarrow{\nabla} U_1 \xrightarrow{\nabla^\perp \cdot} U_2, \quad (2.15)$$

where  $U_0 \subset H^1$ ,  $U_1 \subset H(\text{curl})$ , and  $U_2 \subset L^2$ . In three dimensions, the complex takes the form

$$U_0 \xrightarrow{\nabla} U_1 \xrightarrow{\nabla \times} U_2 \xrightarrow{\nabla \cdot} U_3, \quad (2.16)$$

where  $U_0 \subset H^1$ ,  $U_1 \subset H(\text{curl})$ ,  $U_2 \subset H(\text{div})$ , and  $U_3 \subset L^2$ .

Given an existing two-dimensional complex  $(U_0, U_1, U_2)$  and a one-dimensional complex  $(V_0, V_1)$ , we can generate a product complex on the three-dimensional product cell:

$$W_0 \xrightarrow{\nabla} W_1 \xrightarrow{\nabla \times} W_2 \xrightarrow{\nabla \cdot} W_3, \quad (2.17)$$

where

$$W_0 := U_0 \otimes V_0, \quad (2.18)$$

$$W_1 := \text{HCurl}(U_0 \otimes V_1) \oplus \text{HCurl}(U_1 \otimes V_0), \quad (2.19)$$

$$W_2 := \text{HDiv}(U_1 \otimes V_1) \oplus \text{HDiv}(U_2 \otimes V_0), \quad (2.20)$$

$$W_3 := U_2 \otimes V_1, \quad (2.21)$$

with  $W_0 \subset H^1, W_1 \subset H(\text{curl}), W_2 \subset H(\text{div}), W_3 \subset L^2$  (compare the complex given in Eq. (2.16)). The vector-valued spaces are direct sums of ‘product’ spaces that have been modified by the  $\text{HCurl}$  or  $\text{HDiv}$  operator.

Similarly, taking the product of two one-dimensional complexes produces a product complex on the two-dimensional product cell in which the vector-valued space is in *either*  $H(\text{div})$  or  $H(\text{curl})$ .

## 2.6 Product complexes using differential forms

This section summarises Arnold et al. (2014) by restating the results of subsection 2.4 and subsection 2.5 in the language of differential forms, which can be considered a generalisation of scalar and vector fields.

In three dimensions, 0-forms and 3-forms are identified with scalar fields, while 1-forms and 2-forms are identified with vector fields. In two dimensions, 0-forms and 2-forms are identified with scalar fields. 1-forms are identified with vector fields, but this can be done in two different ways since 1-forms and  $(n-1)$ -forms coincide. This results in two possible vector fields, which differ by a 90-degree rotation. In one dimension, both 0-forms and 1-forms are conventionally identified with scalar fields.

Let  $K_A \subset \mathbb{R}^n, K_B \subset \mathbb{R}^m$  be domains. Suppose we are given de Rham subcomplexes on  $K_A$  and  $K_B$ ,

$$U_0 \xrightarrow{d} U_1 \xrightarrow{d} \cdots \xrightarrow{d} U_n, \quad V_0 \xrightarrow{d} V_1 \xrightarrow{d} \cdots \xrightarrow{d} V_m, \quad (2.22)$$

where each  $U_k$  is a space of (polynomial) differential  $k$ -forms on  $K_A$  and each  $V_k$  is a space of differential  $k$ -forms on  $K_B$ . The product of these complexes is a de Rham subcomplex on  $K_A \times K_B$ :

$$(U \otimes V)_0 \xrightarrow{d} (U \otimes V)_1 \xrightarrow{d} \cdots \xrightarrow{d} (U \otimes V)_{n+m}, \quad (2.23)$$

where, for  $k = 0, 1, \dots, n+m$ ,

$$(U \otimes V)_k := \bigoplus_{i+j=k} (U_i \otimes V_j). \quad (2.24)$$

Note that  $(U \otimes V)_k$  is a space of (polynomial)  $k$ -forms on  $K_A \otimes K_B$ , and can hence be interpreted as a scalar or vector field in 2 or 3 spatial dimensions. It can be easily verified that the definitions in Eqs. (2.23) and (2.24) gives rise to Eq. (2.17) in three dimensions, for example. The discussion in subsection 2.4.2 and subsection 2.4.4 on the product of function spaces can be summarised by the definition of  $\otimes$  on the right-hand side of Eq. (2.24), along with the definition of the standard wedge product of differential forms. It is clear that much of the apparent complexity of the  $\text{HDiv}$  and  $\text{HCurl}$  operators introduced in subsection 2.4 arises from working with scalars and vectors rather than introducing differential forms!

### 3 Implementation

The symbolic operations on finite elements, derived in the previous section, have been implemented within Firedrake (Rathgeber et al., 2015; Rathgeber, 2014). Firedrake is an “*automated system for the portable solution of partial differential equations using the finite element method*”. Firedrake has several dependencies. Some of these are components of the FEniCS Project (Logg et al., 2012a):

**FIAT** FFinite element Automatic Tabulator (Kirby, 2004, 2012), for the construction and tabulation of finite element basis functions

**UFL** Unified Form Language (Alnæs et al., 2014; Alnæs, 2012), a domain-specific language for the specification of finite element variational forms

Firedrake also relies on PyOP2 (Rathgeber et al., 2012) and COFFEE (Luporini et al., 2015).

The changes required to effect the generation of product elements were largely confined to FIAT and UFL, while support for integration over product cells is included in Firedrake’s form compiler. We begin this section with more detailed expositions on FIAT and UFL. We discuss the implementation of product finite elements in subsection 3.3. We talk about the resulting algebraic structure in subsection 3.4. We finish by discussing the new integration regions, in subsection 3.5.

#### 3.1 FIAT

This component is responsible for computing finite element basis functions for a wide range of finite element families. To do this, it works with an abstraction based on Ciarlet’s definition of a finite element, as given in subsection 2.1. The reference cell  $K$  is defined using a set of vertices, with higher-dimensional geometrical objects defined as sets of vertices. The polynomial space  $P$  is defined implicitly through a *prime* basis: typically an orthonormal set of polynomials, such as (on triangles) a Dubiner basis, which can be stably evaluated to high polynomial order. The set of nodes  $N$  is also defined; this implies the existence of a *nodal* basis for  $P$ , as explained previously.

The nodal basis, which is important in calculations, can be expressed as linear combinations of prime basis functions. This is done automatically by FIAT; details are given in Kirby (2004). The main method of interacting with FIAT is by requesting the tabulated values of the nodal basis functions at a set of points inside  $K$  – typically a set of quadrature points. FIAT also stores the geometric decomposition of nodes relative to the topological entities of  $K$ .

#### 3.2 UFL

This component is a domain-specific language, embedded in Python, for representing weak formulations of partial differential equations. It is centred around expressing multilinear forms: maps from the product of some set of function spaces  $\{V_j\}_{j=1}^p$  into the real numbers which are

linear in each argument, where  $\rho$  is 0, 1 or 2. Additionally, the form may be parameterised over one or more *coefficient functions*, and is not necessarily linear in these. The form may include derivatives of functions, and the language has extensive support for matrix algebra operations.

We can assume that the function spaces are finite element spaces; in UFL, these are represented by the `FiniteElement` class. This requires three pieces of information: the element family, the geometric cell, and the polynomial degree. A limited amount of symbolic manipulation on `FiniteElement` objects could already be done: the `UFL EnrichedElement` class is used to represent the  $\oplus$  operator discussed in subsection 2.2.

### 3.3 Implementation of product finite elements

To implement product finite elements, additions to UFL and FIAT were required. The UFL changes are purely symbolic and allow the new elements to be represented. The FIAT changes allow the new elements (and derivatives thereof) to be numerically tabulated at specified points in the reference cell.

As discussed in subsection 2.4.5, we implemented several new element classes in UFL. The existing UFL `FiniteElement` classes has two essential properties: the `degree` and the `value_shape`. The `degree` is the maximal degree of any polynomial basis function – this allows determination of an appropriate quadrature rule. The `value_shape` represents whether the element is scalar-valued or vector-valued and, if applicable, the dimension of the vector in *physical* space. This allows suitable code to be generated when doing vector and tensor operations.

For `TensorProductElements`, we define the `degree` to be a tuple; the basis functions are products of polynomials in distinct sets of variables. It is therefore advantageous to store the polynomial degrees separately for later use with a product quadrature rule. The `value_shape` is defined according to the definition in subsection 2.4.2 for the product of functions. For `HCurl` and `HDiv` elements, the `degree` is identical to the `degree` of the underlying `TensorProductElement`. The `value_shape` needs to be modified: in physical space, these vector-valued elements have dimension equal to the dimension of the physical space.

The secondary role of FIAT is to store a representation of the geometric decomposition of nodes. For product elements, the generation of this was described in subsection 2.4.3. The primary role is to tabulate finite element basis functions, and derivatives thereof, at specified points in the reference cell. The `tabulate` method of a FIAT finite element takes two arguments: the maximal `order` of derivatives to tabulate, and the set of `points`.

Let  $\Phi_{i,j}(x,y,z) := \Phi_i^{(A)}(x,y)\Phi_j^{(B)}(z)$  be some product element basis function; we will assume that this is scalar-valued to ease the exposition. Suppose we need to tabulate the  $x$ -derivative of this at some specified point  $(x_0, y_0, z_0)$ . Clearly

$$\frac{\partial \Phi_{i,j}}{\partial x}(x_0, y_0, z_0) = \frac{\partial \Phi_i^{(A)}}{\partial x}(x_0, y_0)\Phi_j^{(B)}(z_0). \quad (3.1)$$



In other words, the value can be obtained from tabulating (derivatives of) basis functions of the constituent elements at appropriate points. It is clear that this extends to other combinations of derivatives, as well as to components of vector-valued basis functions. Further modifications to the tabulation for curl- or div-conforming vector elements are relatively simple, as detailed in subsection 2.4.4.

### 3.4 Algebraic structure

The extensions described in subsection 3.3 enable sophisticated manipulation of finite elements within UFL. For example, consider the following complex on triangles, highlighted by Cotter and Shipton (2012) as being relevant for numerical weather prediction:

$$P_2 \oplus B_3 \xrightarrow{\nabla^\perp} \text{BDFM}_2 \xrightarrow{\nabla \cdot} \text{DP}_1. \quad (3.2)$$

Here,  $P_2 \oplus B_3$  denotes the space of quadratic polynomials enriched by a cubic ‘bubble’ function,  $\text{BDFM}_2$  represents a member of the vector-valued Brezzi–Douglas–Fortin–Marini element family (Brezzi and Fortin, 1991) in  $H(\text{div})$ , and  $\text{DP}_1$  represents the space of discontinuous, piecewise-linear functions. Suppose we wish to take the product of this with some complex on intervals, such as

$$P_2 \xrightarrow{\frac{d}{dx}} \text{DP}_1. \quad (3.3)$$

This generates a complex on triangular prisms:

$$W_0 \xrightarrow{\nabla} W_1 \xrightarrow{\nabla \times} W_2 \xrightarrow{\nabla \cdot} W_3, \quad (3.4)$$

where

$$W_0 := (P_2^\Delta \oplus B_3^\Delta) \otimes P_2, \quad (3.5)$$

$$W_1 := \text{HCurl}((P_2^\Delta \oplus B_3^\Delta) \otimes \text{DP}_1) \oplus \text{HCurl}(\text{BDFM}_2^\Delta \otimes P_2), \quad (3.6)$$

$$W_2 := \text{HDiv}(\text{BDFM}_2^\Delta \otimes \text{DP}_1) \oplus \text{HDiv}(\text{DP}_1^\Delta \otimes P_2), \quad (3.7)$$

$$W_3 := \text{DP}_1^\Delta \otimes \text{DP}_1; \quad (3.8)$$

we have marked the elements on triangles by  $\Delta$  for clarity. Following our extensions to UFL, the product complex may be constructed as shown in Listing 1. Some of these elements are used in the example in subsection 4.2.

### 3.5 Support for new integration regions

On simplicial meshes, Firedrake supports three types of integrals: integrals over cells, integrals over exterior facets and integrals over interior facets. Integrals over exterior facets are typically used to apply boundary conditions weakly, while integrals over interior facets are used to couple neighbouring cells when discontinuous function spaces are present. The implementation of the

Listing 1: Construction of a complicated product complex in UFL

```

U0_0 = FiniteElement("P", triangle, 2)
U0_1 = FiniteElement("B", triangle, 3)
U0 = EnrichedElement(U0_0, U0_1)
U1 = FiniteElement("BDFM", triangle, 2)
U2 = FiniteElement("DP", triangle, 1)

V0 = FiniteElement("P", interval, 1)
V1 = FiniteElement("DP", interval, 0)

W0 = TensorProductElement(U0, V0)
W1_h = TensorProductElement(U1, V0)
W1_v = TensorProductElement(U0, V1)
W1 = EnrichedElement(HCurl(W1_h), HCurl(W1_v))
W2_h = TensorProductElement(U1, V1)
W2_v = TensorProductElement(U2, V0)
W2 = EnrichedElement(HDiv(W2_h), HDiv(W2_v))
W3 = TensorProductElement(U2, V1)

```

different types of integral is quite elegant: the only difference between integrating a function over the interior of the cell and over a single facet is the choice of quadrature points and quadrature weights. Note that Firedrake assumes that the mesh is conforming – hanging nodes are not currently supported.

On product cells, all entities can be considered as a product of entities on the constituent cells. We can therefore construct product quadrature rules, making use of existing quadrature rules for constituent cells and facets thereof. In addition, we split the facet integrals into separate integrals over ‘vertical’ and ‘horizontal’ facets. This is natural when executing a computational kernel over an extruded unstructured mesh, and may be useful in geophysical contexts where horizontal and vertical motions may be treated differently.

## 4 Numerical examples

In this section, we give several examples to demonstrate the correctness of our implementation. Quantitative analysis is performed where possible, e.g. demonstration of convergence to a known solution at expected order with increasing mesh resolution. Tests are performed in both two and three spatial dimensions. We make use of Firedrake’s `ExtrudedMesh` functionality. In two dimensions, the cells are quadrilaterals, usually squares. In three dimensions, we use triangular prisms, though we can also build elements on hexahedra.

When referring to standard finite element spaces, we follow the convention in which the number refers to the degree of the minimal complete polynomial space containing the element, not the maximal complete polynomial space contained by the element. Thus, an element containing some, but not all, linear polynomials is numbered 1, rather than 0. This is the convention used by UFL, and is also justified from the perspective of finite element exterior calculus.

## 4.1 Vector Laplacian (3D)

We seek a solution to

$$-\nabla(\nabla \cdot \vec{u}) + \nabla \times (\nabla \times \vec{u}) = \vec{f} \quad (4.1)$$

in a domain  $\Omega$ , with boundary conditions

$$\vec{u} \cdot \vec{n} = 0, \quad (4.2)$$

$$(\nabla \times \vec{u}) \times \vec{n} = 0 \quad (4.3)$$

on  $\partial\Omega$ , where  $\vec{n}$  is the outward normal. A naïve discretisation can lead to spurious solutions, especially on non-convex domains, but an accurate discretisation can be obtained by introducing an auxiliary variable (see, for example, Arnold et al. (2010)):

$$\sigma = -\nabla \cdot \vec{u}, \quad (4.4)$$

$$\nabla \sigma + \nabla \times (\nabla \times \vec{u}) = \vec{f}. \quad (4.5)$$

Let  $V_0 \subset H^1$ ,  $V_1 \subset H(\text{curl})$  be finite element spaces. A suitable weak formulation is: find  $\sigma \in V_0$ ,  $\vec{u} \in V_1$  such that

$$\langle \tau, \sigma \rangle - \langle \nabla \tau, \vec{u} \rangle = 0, \quad (4.6)$$

$$\langle \vec{v}, \nabla \sigma \rangle + \langle \nabla \times \vec{v}, \nabla \times \vec{u} \rangle = \langle \vec{v}, \vec{f} \rangle, \quad (4.7)$$

for all  $\tau \in V_0$ ,  $\vec{v} \in V_1$ , where we have used angled brackets to denote the standard  $L^2$  inner product. The boundary conditions have been implicitly applied, in a weak sense, through neglecting the surface terms when integrating by parts.

We take  $\Omega$  to be the unit cube  $[0, 1]^3$ . Let  $k$ ,  $l$  and  $m$  be arbitrary. Then

$$\vec{f} = \pi^2 \begin{pmatrix} (k^2 + l^2) \sin(k\pi x) \cos(l\pi y) \\ (l^2 + m^2) \sin(l\pi y) \cos(m\pi z) \\ (k^2 + m^2) \sin(m\pi z) \cos(k\pi x) \end{pmatrix} \quad (4.8)$$

produces the solution

$$\vec{u} = \begin{pmatrix} \sin(k\pi x) \cos(l\pi y) \\ \sin(l\pi y) \cos(m\pi z) \\ \sin(m\pi z) \cos(k\pi x) \end{pmatrix}, \quad (4.9)$$

which satisfies the boundary conditions.

To discretise this problem, we subdivide  $\Omega$  into triangular prisms whose base is a right-angled triangle with short sides of length  $\Delta x$  and whose height is  $\Delta x$ . We use the  $Q_r$  prism element for the  $H^1$  space, and the degree- $r$  Nédélec prism element of the first kind for the  $H(\text{curl})$  space, for  $r$  from 1 to 3. We take  $k$ ,  $l$  and  $m$  to be 1, 2 and 3, respectively. We approximate  $\vec{f}$  by interpolating the analytic expression onto a vector-valued function in  $Q_{r+1}$ . The  $L^2$  errors between the calculated and ‘analytic’ solutions for varying  $\Delta x$  are plotted in Figure 1. This is done for both  $\vec{u}$  and  $\sigma$ ; the so-called analytic solutions are approximations which are formed by interpolating the genuine analytic solution onto nodes of  $Q_{r+1}$ .

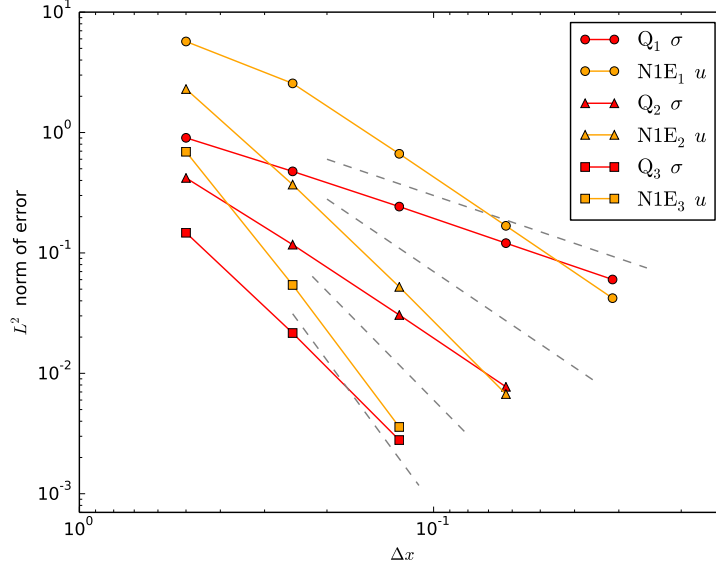


Figure 1: The  $L^2$  error between the computed and ‘analytic’ solution is plotted against  $\Delta x$  for the 3D problem described in subsection 4.1. The dotted lines are proportional to  $\Delta x^n$ , for  $n$  from 1 to 4, and are merely to aid comprehension.

## 4.2 Gravity wave (3D)

A simple model of atmospheric flow is given by

$$\frac{\partial \vec{u}}{\partial t} = -\nabla p + b\hat{z}, \quad \frac{\partial b}{\partial t} = -N^2 \vec{u} \cdot \hat{z}, \quad \frac{\partial p}{\partial t} = -c^2 \nabla \cdot \vec{u}, \quad (4.10)$$

along with the boundary condition  $\vec{u} \cdot \vec{n} = 0$ , where  $\vec{n}$  is a unit normal vector. The prognostic variables are the velocity,  $\vec{u}$ , the pressure perturbation,  $p$ , and the buoyancy perturbation,  $b$ . The scalars  $N$  and  $c$  are (dimensional) constants, while  $\hat{z}$  represents a unit vector opposite to the direction of gravity. These equations are a reduction of, for example, (17)–(21) from Skamarock and Klemp (1994), in which we have neglected the constant background velocity and the Coriolis term, and rescaled  $\theta$  by  $\theta_0/g$  to produce  $b$ .

Given some three-dimensional product complex as in Eq. (2.17), we seek a solution with  $\vec{u} \in W_2^0$ ,  $b \in W_2^v$  and  $p \in W_3$ .  $W_2^0$  is the subspace of  $W_2$  whose normal component vanishes on the boundary of the domain.  $W_2^v$  denotes the ‘‘vertical’’ part of  $W_2$ : if we write  $W_2$  as a sum of two product elements  $\text{HDiv}(U_1 \otimes V_1)$  and  $\text{HDiv}(U_2 \otimes V_0)$  then  $W_2^v$  is the *scalar-valued* product  $U_2 \otimes V_0$ , as was constructed in Listing 1. This combination of finite element spaces for  $\vec{u}$  and  $b$  is analogous to the Charney–Phillips staggering of variables in the vertical direction (Charney and Phillips, 1953).

A semi-discrete form of (4.10) is the following: find  $\vec{u} \in W_2^0$ ,  $b \in W_2^v$ ,  $p \in W_3$  such that for all

$$\vec{w} \in W_2^0, \gamma \in W_2^v, \phi \in W_3$$

$$\left\langle \vec{w}, \frac{\partial \vec{u}}{\partial t} \right\rangle - \langle \nabla \cdot \vec{w}, p \rangle - \langle \vec{w}, b \hat{z} \rangle = 0 \quad (4.11)$$

$$\left\langle \gamma, \frac{\partial b}{\partial t} \right\rangle + N^2 \langle \gamma, \vec{u} \cdot \hat{z} \rangle = 0 \quad (4.12)$$

$$\left\langle \phi, \frac{\partial p}{\partial t} \right\rangle + c^2 \langle \phi, \nabla \cdot \vec{u} \rangle = 0. \quad (4.13)$$

It can be easily verified that the original equations, (4.10), together with the boundary condition lead to conservation of the energy perturbation

$$\int_{\Omega} \frac{1}{2} |\vec{u}|^2 + \frac{1}{2N^2} b^2 + \frac{1}{2c^2} p^2 \, dx. \quad (4.14)$$

The three terms can be interpreted as kinetic energy (KE), potential energy (PE) and internal energy (IE), respectively. The semi-discretisation given in Eqs. (4.11)–(4.13) also conserves this energy. If we discretise in time using the implicit midpoint rule, which preserves quadratic invariants (Leimkuhler and Reich, 2005) then the fully discrete system will conserve energy as well.

We take the domain to be a spherical shell centred at the origin. Its inner radius,  $a$ , is approximately 6371km, and its thickness,  $H$ , is 10km. The domain is divided into triangular prism cells with side-lengths of the order of 1000km and height 1km. We take  $N = 10^{-2} \text{s}^{-1}$  and  $c = 300 \text{ms}^{-1}$ . The simulation starts at rest with a buoyancy perturbation and a vertically balancing pressure field given by

$$b = \frac{\sin(\pi(|\vec{x}| - a)/H)}{1 + z^2/L^2}, \quad p = -\frac{H \cos(\pi(|\vec{x}| - a)/H)}{\pi (1 + z^2/L^2)}; \quad (4.15)$$

$L$  is a horizontal length-scale, which we take to be 500km. We use a timestep of 1920s, and run for a total of 480,000s.

To discretise this problem, we use the product elements formed from the BDFM<sub>2</sub> complex on triangles and the P<sub>2</sub>–DP<sub>1</sub> complex on intervals; these were constructed in subsection 3.4. The initial conditions are interpolated into the buoyancy and pressure fields. The energy is calculated at every time step; the results are plotted in Figure 2. The total energy is conserved to roughly one part in  $1.4 \times 10^8$ , which is comparable to the linear solver tolerances.

### 4.3 DG advection (2D)

The advection of a scalar field  $q$  by a known divergence-free velocity field  $\vec{u}_0$  can be described by the equation

$$\frac{\partial q}{\partial t} + \nabla \cdot (\vec{u}_0 q) = 0. \quad (4.16)$$

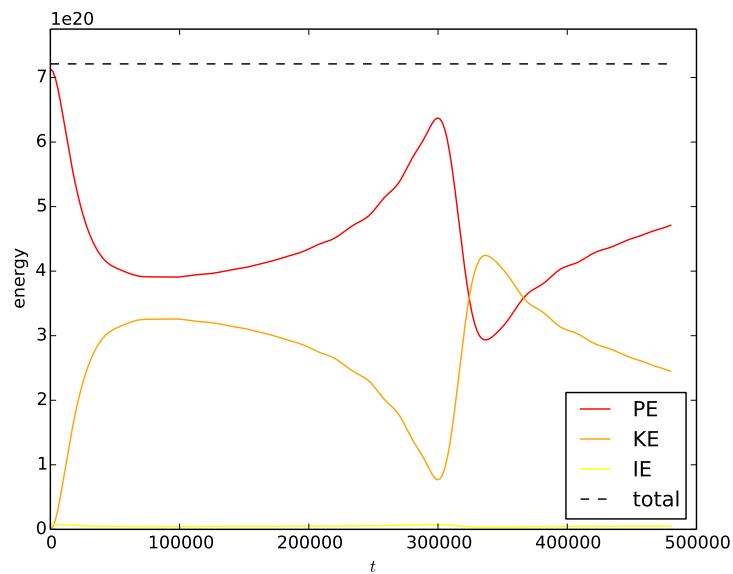


Figure 2: Evolution of energy for the simulation described in subsection 4.2. The components are the potential energy, PE, the kinetic energy, KE, and the internal energy, IE. The choice of spatial and temporal discretisations leads to exact conservation of total energy up to solver tolerances; this is indeed observed. The event at approximately  $t = 320,000$ s corresponds to the zonally-symmetric gravity wave reaching the poles of the spherical domain.

If  $q$  is in a discontinuous function space,  $V$ , a suitable weak formulation is

$$\left\langle \phi, \frac{\partial q}{\partial t} \right\rangle = \langle \nabla \phi, q \vec{u}_0 \rangle - \int_{\Gamma_{\text{ext}}} \phi \tilde{q} \vec{u}_0 \cdot \vec{n} \, ds - \int_{\Gamma_{\text{int}}} \llbracket \phi \rrbracket \tilde{q} \vec{u}_0 \cdot \vec{n} \, dS, \quad (4.17)$$

for all  $\phi \in V$ , where the integrals on the right hand side are over *exterior* and *interior* mesh facets, with  $ds$  and  $dS$  appropriate integration measures.  $\vec{n}$  is the appropriately-oriented normal vector,  $\tilde{q}$  represents the *upwind* value of  $q$ , while  $\llbracket \phi \rrbracket$  represents the jump in  $\phi$ . We assume that, on parts of the boundary corresponding to inflow,  $\tilde{q} = 0$ . This example will therefore demonstrate the ability to integrate over interior and exterior mesh facets.

We discretise Eq. (4.17) in time using the third-order three-stage strong-stability-preserving Runge-Kutta scheme given in Shu and Osher (1988). We take  $\Omega$  to be the unit square  $[0, 1]^2$ . Our initial condition will be a cosine hill

$$q = \begin{cases} \frac{1}{2} \left( 1 + \cos \left( \pi \frac{|\vec{x} - \vec{x}_0|}{r_0} \right) \right), & |\vec{x} - \vec{x}_0| < r_0 \\ 0, & \text{otherwise,} \end{cases} \quad (4.18)$$

with radius  $r_0 = 0.15$ , centred at  $\vec{x}_0 = (0.25, 0.5)$ . The prescribed velocity field is

$$\vec{u}_0(\vec{x}, t) = \cos \left( \frac{\pi t}{T} \right) \begin{pmatrix} \sin(\pi x)^2 \sin(2\pi y) \\ -\sin(\pi y)^2 \sin(2\pi x) \end{pmatrix}, \quad (4.19)$$

as in LeVeque (1996). This gives a reversing, swirling flow field which vanishes on the boundaries of  $\Omega$ . The initial condition should be recovered at  $t = T$ . Following (LeVeque, 1996), we take  $T = \frac{3}{2}$ .

To discretise this problem, we subdivide  $\Omega$  into squares with side length  $\Delta x$ . We use  $DQ_r$  for the discontinuous function space, for  $r$  from 0 to 2, which are products of 1D discontinuous elements. We initialise  $q$  by interpolating the expression given in Eq. (4.18) into the appropriate space. We approximate  $\vec{u}_0$  by interpolating the expression given in Eq. (4.19) onto a vector-valued function in  $Q_2$ . The  $L^2$  errors between the initial and final  $q$  fields for varying  $\Delta x$  are plotted in Figure 3.

## 5 Limitations and extensions

There are several limitations of the current implementation, which leaves scope for future work. The most obvious is that the quadrature calculations are relatively inefficient, particularly at high order. The product structure of the basis functions can be exploited to generate a more efficient implementation of numerical quadrature. This can be done using the *sum-factorisation* method, which lifts invariant terms out of the innermost loop. In the very simplest cases, direct factorisation of the integral may be possible. Such operations could have been implemented within Firedrake's form compiler. However, this would mask the underlying issue – that FIAT, which is supposed to be wholly responsible for producing the finite elements, has no way to communicate any underlying basis function structure. Work is underway on a more sophisticated

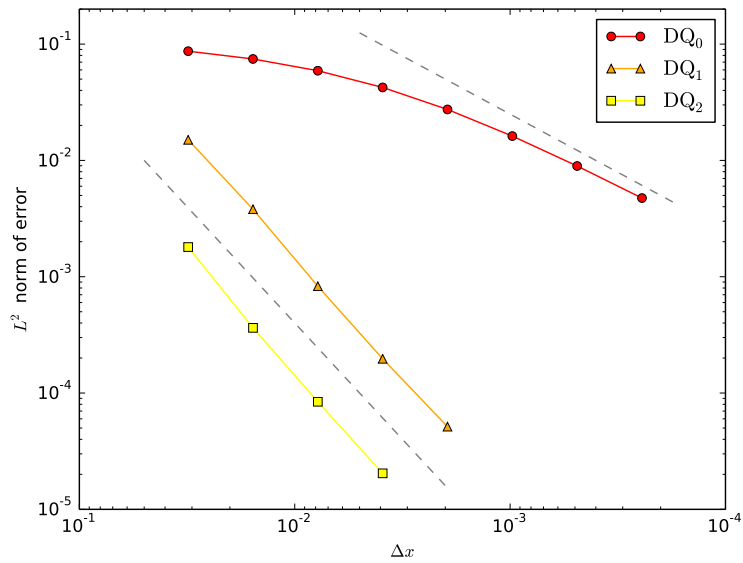


Figure 3: The  $L^2$  error between the computed and ‘analytic’ solution is plotted against  $\Delta x$  for the problem described in subsection 4.3. The dotted lines are proportional to  $\Delta x$  and  $\Delta x^2$ , and are merely to aid comprehension. The  $DQ_0$  simulations converge at first-order for sufficiently small values of  $\Delta x$ . The  $DQ_1$  simulations converge at second-order, as expected. The cosine bell initial condition has a discontinuous second derivative, which inhibits the  $DQ_2$  simulations from exceeding a second-order rate of convergence.



layer of software that returns an *algorithm* for performing a given operation on a finite element, rather than merely an array of tabulated basis functions.

Firedrake has recently gained full support for non-affine coordinate transformations. In the *previous* version of the form compiler, the Jacobian of the coordinate mapping was assumed to be constant across each cell. This is satisfactory for simplices, since the physical and reference cells can always be linked by an affine transformation. However, this statement does not hold for quadrilateral, triangular prism, or hexahedral cells. Firedrake now evaluates the Jacobian at quadrature points. This functionality is also necessary for accurate calculations on curvilinear cells, in which the coordinate transformation is quadratic or higher-order. This allows, for example, more faithful representations of a sphere or spherical shell, extending the work done in Rognes et al. (2013).

## 6 Conclusion

This paper presented extensions to the automated code generation pipeline of Firedrake to facilitate the use of finite element spaces on non-simplex cells, in two and three dimensions. A wide range of finite elements can be constructed, including, but not limited to, those listed in Table 3. The examples made extensive use of the recently-added extruded mesh functionality in Firedrake; a related paper detailing the implementation of extruded meshes is in preparation.

All numerical experiments given in this paper were performed with the following versions of software, which we have archived on Zenodo: Firedrake (Mitchell et al., 2016), PyOP2 (Rathgeber et al., 2016), TSFC (Homolya and Mitchell, 2016), COFFEE (Luporini et al., 2016), UFL (Alnæs et al., 2016), FIAT (Rognes et al., 2016), PETSc (Smith et al., 2016), PETSc4py (Dalcin et al., 2016). The code for the numerical experiments can be found in the supplement to the paper.

## Acknowledgements

Andrew McRae wishes to acknowledge funding and other support from the Grantham Institute and Climate-KIC. This work was supported by the Natural Environment Research Council [grant numbers NE/K006789/1, NE/K008951/1], and an Engineering and Physical Sciences Research Council prize studentship.

## References

MFEM: Modular finite element methods. <http://mfem.org>.

Martin S. Alnæs, Anders Logg, Kristian B. Ølgaard, Marie E. Rognes, and Garth N. Wells. Unified Form Language: A domain-specific language for weak formulations of partial differ-

Table 3: Examples of the construction of standard finite element spaces. In the left-hand column, we use the notation of the *Periodic Table of the Finite Elements (Arnold and Logg, 2014)* where possible.

Element	Cell	Construction*
$Q_r$ (also written $Q_{r,r}$ )	quadrilateral	$P_r \otimes P_r$
$RTCE_r$ , Raviart–Thomas ‘edge’ element <sup>†</sup>	quadrilateral	$\text{HCurl}(P_r \otimes DP_{r-1}) \oplus \text{HCurl}(DP_{r-1} \otimes P_r)$
Nédélec ‘edge’ element of the second kind <sup>‡</sup>	quadrilateral	$\text{HCurl}(P_r \otimes DP_r) \oplus \text{HCurl}(DP_r \otimes P_r)$
$RTCF_r$ , Raviart–Thomas ‘face’ element (Raviart and Thomas, 1977)	quadrilateral	$\text{HDiv}(P_r \otimes DP_{r-1}) \oplus \text{HDiv}(DP_{r-1} \otimes P_r)$
Nédélec ‘face’ element of the second kind <sup>‡</sup>	quadrilateral	$\text{HDiv}(P_r \otimes DP_r) \oplus \text{HDiv}(DP_r \otimes P_r)$
$DQ_r$ (discontinuous $Q_r$ )	quadrilateral	$DP_r \otimes DP_r$
$P_{r,r}$ <sup>††</sup>	triangular prism	$P_r^\Delta \otimes P_r$
Nédélec ‘edge’ element of the first kind <sup>‡‡</sup>	triangular prism	$\text{HCurl}(P_r^\Delta \otimes DP_{r-1}) \oplus \text{HCurl}(\text{RTE}_r^\Delta \otimes P_r)$
Nédélec ‘edge’ element of the second kind (Nédélec, 1986)	triangular prism	$\text{HCurl}(P_r^\Delta \otimes DP_r) \oplus \text{HCurl}(\text{BDME}_r^\Delta \otimes P_r)$
Nédélec ‘face’ element of the first kind <sup>‡‡</sup>	triangular prism	$\text{HDiv}(\text{RTF}_r^\Delta \otimes DP_{r-1}) \oplus \text{HDiv}(DP_{r-1}^\Delta \otimes P_r)$
Nédélec ‘face’ element of the second kind (Nédélec, 1986)	triangular prism	$\text{HDiv}(\text{BDMF}_r^\Delta \otimes DP_r) \oplus \text{HDiv}(DP_r^\Delta \otimes P_r)$
$DP_{r,r}$	triangular prism	$DP_r^\Delta \otimes DP_r$
$Q_r$ (also written $Q_{r,r,r}$ )	hexahedra	$Q_r^\square \otimes P_r$
$NCE_r$ , Nédélec ‘edge’ element of the first kind (Nédélec, 1980)	hexahedra	$\text{HCurl}(Q_r^\square \otimes DP_{r-1}) \oplus \text{HCurl}(\text{RTCE}_r^\square \otimes P_r)$
Nédélec ‘edge’ element of the second kind (Nédélec, 1986)	hexahedra	$\text{HCurl}(Q_r^\square \otimes DP_r) \oplus \text{HCurl}(\text{N2CE}_r^\square \otimes P_r)$
$NCF_r$ , Nédélec ‘face’ element of the first kind (Nédélec, 1980)	hexahedra	$\text{HDiv}(\text{RTCF}_r^\square \otimes DP_{r-1}) \oplus \text{HDiv}(\text{DQ}_{r-1}^\square \otimes P_r)$
Nédélec ‘face’ element of the second kind (Nédélec, 1986)	hexahedra	$\text{HDiv}(\text{N2CF}_r^\square \otimes DP_r) \oplus \text{HDiv}(\text{DQ}_r^\square \otimes P_r)$
$DQ_r$	hexahedra	$\text{DQ}_r^\square \otimes DP_r$

<sup>†</sup>: this is a curl-conforming analogue of the usual Raviart–Thomas quadrilateral element (Raviart and Thomas, 1977).

<sup>‡</sup>: these are the quadrilateral reductions of the hexahedral Nédélec elements of the second kind (Nédélec, 1986).

<sup>††</sup>: this denotes the element with polynomial degree  $r$  in the first two variables, and polynomial degree  $r$  in the third variable separately.

<sup>‡‡</sup>: these are the prism equivalents of the tetrahedral and hexahedral Nédélec elements (Nédélec, 1980).

\*: RTE and RTF refer to the Raviart–Thomas edge and face elements on triangles. BDME and BDMF refer to the Brezzi–Douglas–Marini (Brezzi et al., 1985) edge and face elements on triangles. N2CE and N2CF refer to the Nédélec elements of the second kind that we construct on quadrilaterals.

- ential equations. *ACM Transactions on Mathematical Software*, 40(2):9:1–9:37, 2014. ISSN 0098-3500. doi: 10.1145/2566630.
- Martin Sandve Alnæs. UFL: a finite element form language. In *Automated Solution of Differential Equations by the Finite Element Method*, volume 84 of *Lecture Notes in Computational Science and Engineering*, pages 303–338. Springer, 2012. doi: 10.1007/978-3-642-23099-8\_17.
- Martin Sandve Alnæs, Anders Logg, Andrew T. T. McRae, Garth N. Wells, Marie E. Rognes, Lawrence Mitchell, Miklós Homolya, Kristian B. Ølgaard, Aslak Bergersen, Johannes Ring, David A. Ham, Chris Richardson, Kent-Andre Mardal, Jan Blechta, Florian Rathgeber, Graham Markall, Colin J. Cotter, Lizao Li, Matthias Liertzer, Maximilian Albert, Johan Hake, and Tuomas Airaksinen. UFL: The Unified Form Language, February 2016.
- Douglas N. Arnold and Gerard Awanou. Finite element differential forms on cubical meshes. *Mathematics of Computation*, 83(288):1551–1570, 2014. ISSN 0025-5718. doi: 10.1090/S0025-5718-2013-02783-4.
- Douglas N. Arnold and Anders Logg. Periodic table of the finite elements. *SIAM News*, November 2014. URL <http://femtable.org>.
- Douglas N. Arnold, Richard S. Falk, and Ragnar Winther. Finite element exterior calculus, homological techniques, and applications. *Acta Numerica*, 15:1–155, 2006. ISSN 1474-0508. doi: 10.1017/S0962492906210018.
- Douglas N. Arnold, Richard S. Falk, and Ragnar Winther. Finite element exterior calculus: from Hodge theory to numerical stability. *Bulletin (New Series) of the American Mathematical Society*, 47(2):281–354, 2010. ISSN 0273-0979. doi: 10.1090/S0273-0979-10-01278-4.
- Douglas N. Arnold, Daniele Boffi, and Francesca Bonizzoni. Finite element differential forms on curvilinear cubic meshes and their approximation properties. *Numerische Mathematik*, pages 1–20, 2014. ISSN 0029-599X. doi: 10.1007/s00211-014-0631-3.
- Satish Balay, Shrirang Abhyankar, Mark F. Adams, Jed Brown, Peter Brune, Kris Buschelman, Victor Eijkhout, William D. Gropp, Dinesh Kaushik, Matthew G. Knepley, Lois Curfman McInnes, Karl Rupp, Barry F. Smith, and Hong Zhang. PETSc Users Manual. Technical Report ANL-95/11 - Revision 3.5, Argonne National Laboratory, 2014. URL <http://www.mcs.anl.gov/petsc>.
- W. Bangerth, T. Heister, L. Heltai, G. Kanschat, M. Kronbichler, M. Maier, B. Turcksin, and T. D. Young. The deal.II Library, Version 8.2. *Archive of Numerical Software*, 3(1), 2015. ISSN 2197-8263. doi: 10.11588/ans.2015.100.18031.
- Peter Bastian, Felix Heimann, and Sven Marnach. Generic implementation of finite element methods in the Distributed and Unified Numerics Environment (DUNE). *Kybernetika*, 46: 294–315, 2010. ISSN 0023-5954.

- Franco Brezzi and Michel Fortin. *Mixed and Hybrid Finite Element Methods*. Springer Series in Computational Mathematics. Springer-Verlag, New York, 1991. ISBN 0-387-97582-9.
- Franco Brezzi, Jim Douglas, Jr., and L. D. Marini. Two families of mixed finite elements for second order elliptic problems. *Numerische Mathematik*, 47(2):217–235, 1985. ISSN 0029-599X. doi: 10.1007/BF01389710.
- C.D. Cantwell, D. Moxey, A. Comerford, A. Bolis, G. Rocco, G. Mengaldo, D. De Grazia, S. Yakovlev, J.-E. Lombard, D. Ekelschot, B. Jordi, H. Xu, Y. Mohamied, C. Eskilsson, B. Nelson, P. Vos, C. Biotto, R.M. Kirby, and S.J. Sherwin. Nektar++: An open-source spectral/hp element framework. *Computer Physics Communications*, 192:205–219, 2015. ISSN 0010-4655. doi: 10.1016/j.cpc.2015.02.008.
- J. G. Charney and N. A. Phillips. Numerical integration of the quasi-geostrophic equations for barotropic and simple baroclinic flows. *Journal of Meteorology*, 10(2):71–99, 1953. ISSN 0095-9634. doi: 10.1175/1520-0469(1953)010<0071:NIOTQG>2.0.CO;2.
- Philippe G Ciarlet. *The finite element method for elliptic problems*. North-Holland, 1978.
- C. J. Cotter and J. Shipton. Mixed finite elements for numerical weather prediction. *Journal of Computational Physics*, 231:7076–7091, 2012. ISSN 0021-9991. doi: 10.1016/j.jcp.2012.05.020.
- Lisandro Dalcin, Lawrence Mitchell, Jed Brown, Patrick E. Farrell, Michael Lange, Barry Smith, Dmitry Karpeyev, nocollier, Matthew Knepley, David A. Ham, Simon Wolfgang Funke, Aron Ahmadi, Thomas Hirsch, Miklós Homolya, Jorge Cañardo Alastuey, Asbjørn Nilsen Riseth, Garth Wells, and Jonathan Guyer. PETSc4py: The Python interface to PETSc, February 2016.
- Miklós Homolya and Lawrence Mitchell. TSFC: The Two Stage Form Compiler, February 2016.
- Robert C. Kirby. Algorithm 839: FIAT, a new paradigm for computing finite element basis functions. *ACM Trans. Math. Softw.*, 30(4):502–516, 2004. ISSN 0098-3500. doi: 10.1145/1039813.1039820.
- Robert C. Kirby. FIAT: numerical construction of finite element basis functions. In *Automated Solution of Differential Equations by the Finite Element Method*, volume 84 of *Lecture Notes in Computational Science and Engineering*, pages 247–255. Springer, 2012. doi: 10.1007/978-3-642-23099-8\_13.
- Robert C. Kirby and Anders Logg. A compiler for variational forms. *ACM Trans. Math. Softw.*, 32(3):417–444, 2006. ISSN 0098-3500. doi: 10.1145/1163641.1163644.
- Benedict Leimkuhler and Sebastian Reich. *Simulating Hamiltonian Dynamics*, chapter 12. Cambridge University Press, 2005. ISBN 9780521772907. doi: 10.1017/CBO9780511614118.
- Randall J LeVeque. High-resolution conservative algorithms for advection in incompressible flow. *SIAM Journal on Numerical Analysis*, 33(2):627–665, 1996. ISSN 0036-1429. doi: 10.1137/0733033.

- Anders Logg, Kent-Andre Mardal, Garth N. Wells, et al. *Automated Solution of Differential Equations by the Finite Element Method*. Springer, 2012a. ISBN 978-3-642-23098-1. doi: 10.1007/978-3-642-23099-8.
- Anders Logg, Kristian B Ølgaard, Marie E Rognes, and Garth N Wells. FFC: the FEniCS form compiler. In *Automated Solution of Differential Equations by the Finite Element Method*, volume 84 of *Lecture Notes in Computational Science and Engineering*, pages 227–238. Springer, 2012b. doi: 10.1007/978-3-642-23099-8\_11.
- Fabio Luporini, Ana Lucia Varbanescu, Florian Rathgeber, Gheorghe-Teodor Bercea, J. Ramanujam, David A. Ham, and Paul H. J. Kelly. Cross-Loop Optimization of Arithmetic Intensity for Finite Element Local Assembly. *ACM Transactions on Architecture and Code Optimization*, 11(4):57:1–57:25, 2015. ISSN 1544-3566. doi: 10.1145/2687415.
- Fabio Luporini, Lawrence Mitchell, Miklós Homolya, Florian Rathgeber, David A. Ham, Michael Lange, Graham Markall, and Francis Russell. COFFEE: A Compiler for Fast Expression Evaluation, February 2016.
- Lawrence Mitchell, Florian Rathgeber, David A. Ham, Miklós Homolya, Andrew T. T. McRae, Gheorghe-Teodor Bercea, Michael Lange, Colin J Cotter, Christian T. Jacobs, Fabio Luporini, Simon Wolfgang Funke, Anna Kalogirou, Henrik Büsing, Tuomas Kärnä, Hannah Rittich, Eike Hermann Mueller, Stephan Kramer, Graham Markall, Patrick E. Farrell, Asbjørn Nilsen Riseth, Justin Chang, and Geordie McBain. Firedrake: an automated finite element system, February 2016.
- J. C. Nédélec. Mixed finite elements in  $\mathbb{R}^3$ . *Numerische Mathematik*, 35(3):315–341, 1980. ISSN 0029-599X. doi: 10.1007/BF01396415.
- J. C. Nédélec. A new family of mixed finite elements in  $\mathbb{R}^3$ . *Numerische Mathematik*, 50(1): 57–81, 1986. ISSN 0029-599X. doi: 10.1007/BF01389668.
- Kristian B. Ølgaard and Garth N. Wells. Optimisations for quadrature representations of finite element tensors through automated code generation. *ACM Transactions on Mathematical Software*, 37(1):8:1–8:23, 2010. ISSN 0098-3500. doi: 10.1145/1644001.1644009.
- Florian Rathgeber. *Productive and Efficient Computational Science Through Domain-specific Abstractions*. PhD thesis, Imperial College London, July 2014.
- Florian Rathgeber, Graham R. Markall, Lawrence Mitchell, Nicolas Lorient, David A. Ham, Carlo Bertolli, and Paul H.J. Kelly. PyOP2: A high-level framework for performance-portable simulations on unstructured meshes. In *High Performance Computing, Networking Storage and Analysis, SC Companion:*, pages 1116–1123, Los Alamitos, CA, USA, 2012. IEEE Computer Society. ISBN 978-1-4673-3049-7. doi: 10.1109/SC.Companion.2012.134.
- Florian Rathgeber, David A. Ham, Lawrence Mitchell, Michael Lange, Fabio Luporini, Andrew T. T. McRae, Gheorghe-Teodor Bercea, Graham R. Markall, and Paul H. J. Kelly. Firedrake: automating the finite element method by composing abstractions. *Submitted*, 2015.

- Florian Rathgeber, Lawrence Mitchell, Fabio Luporini, Graham Markall, David A. Ham, Gheorghe-Teodor Bercea, Miklós Homolya, Andrew T. T. McRae, Hector Dearman, Christian T. Jacobs, gpts, Simon Wolfgang Funke, kahosato, and Francis Russell. PyOP2: Framework for performance-portable parallel computations on unstructured meshes, February 2016.
- P. A. Raviart and J. M. Thomas. A mixed finite element method for 2nd order elliptic problems. In *Mathematical aspects of finite element methods*, pages 292–315. Springer, 1977. doi: 10.1007/BFb0064470.
- M. E. Rognes, D. A. Ham, C. J. Cotter, and A. T. T. McRae. Automating the solution of pdes on the sphere and other manifolds in FEniCS 1.2. *Geoscientific Model Development*, 6(6): 2099–2119, 2013. ISSN 1991-9603. doi: 10.5194/gmd-6-2099-2013.
- Marie E. Rognes, alogg, Miklós Homolya, David A. Ham, Nico Schlömer, Jan Blechta, Aslak Bergersen, Johannes Ring, Colin J Cotter, Lawrence Mitchell, Garth Wells, Florian Rathgeber, Robert Kirby, LIZAO LI, Martin Sandve Alnæs, Andrew T. T. McRae, and mliertzer. FIAT: The Finite Element Automated Tabulator, February 2016.
- Joachim Schöberl. C++11 Implementation of Finite Elements in NGSolve. *preprint*, 2014.
- Joachim Schöberl and Sabine Zaglmayr. High order Nédélec elements with local complete sequence properties. *COMPEL: The International Journal for Computation and Mathematics in Electrical and Electronic Engineering*, 24(2):374–384, 2005. ISSN 0332-1649. doi: 10.1108/03321640510586015.
- Chi-Wang Shu and Stanley Osher. Efficient implementation of essentially non-oscillatory shock-capturing schemes. *Journal of Computational Physics*, 77(2):439–471, 1988. ISSN 0021-9991. doi: 10.1016/0021-9991(88)90177-5.
- W. C. Skamarock and J. B. Klemp. Efficiency and accuracy of the Klemp-Wilhelmson time-splitting technique. *Monthly Weather Review*, 122(11):2623–2630, 1994. ISSN 0027-0644. doi: 10.1175/1520-0493(1994)122<2623:EAAOTK>2.0.CO;2.
- Barry Smith, Satish Balay, Matthew Knepley, Jed Brown, Lois Curfman McInnes, Hong Zhang, Peter Brune, sarich, Dmitry Karpeyev, Lisandro Dalcin, stefanozampini, markadams, Victor Minden, VictorEijkhout, vijaysm, tisaac, Karl Rupp, SurtaiHan, slepc, Michael Lange, Dominic Meiser, Xuan Zhou, baagaard, dmay23, tmunson, emconsta, Debojyoti Ghosh, Lawrence Mitchell, Patrick Sanan, and bourdin. PETSc: Portable, Extensible Toolkit for Scientific Computation, February 2016.